Chapter 5 Vectorial Field Simulation

5.1 Results of Vectorial Diffraction Integrals

From calculation of vectorial Rayleigh diffraction integrals, the x-, y-, and z-components of the electric field of the optical bottle beam can be obtained by assuming a specific input polarization field. In this work, we used the radial- and x-polarized lights as the input fields. By setting the same physical parameters, namely, the central wavelength and spot size (w_0) of the input Gaussian beam, the distance between lens and axicon (Z_0), and radius of the aperture (R) be 670 nm, 2.4 mm, 72 mm, and 5 mm, respectively, we obtained the bottle ranges of the scalar diffraction (Fresnel-Kirchhoff's diffraction) and the vectorial diffraction (vectorial Rayleigh diffraction) at the condition (1) with $\gamma = 5^0$, $f = 35.08$ mm and condition (2) with $\gamma = 0.5^0$, $f = 5.08$ mm as shown in Table 5.1.

Table 5.1 Results of bottle ranges calculated from the scalar and vectorial diffraction.

Range of bottle beam (mm)	Condition (1): $\gamma = 5^0$, $f = 35.08$ mm	Condition(2): $\gamma = 0.5^0$, $f = 5.08$ mm
Scalar diffraction (ΔZ)	25.6~66.8 (41.2)	5.1~5.4 (0.3)
Vectorial diffraction (ΔZ)	10.8~50.8 (40.0)	3.9~5.4 (1.5)

From Table 5.1, we found although the start positions of bottle beam are different for these two calculation methods, the sizes of bottle beam are the same corresponding to 41.2 mm and 40 mm for condition (1). However, the scalar diffraction gives size of bottle of 0.3 mm and 1.5 mm for the vectorial diffraction. The discrepancy may be due to paraxial approximation in the vectorial diffraction approach for smaller focal length. And the beam profiles in bottle regions for two conditions are also shown in Figure 5.1 and Figure 5.2, respectively.

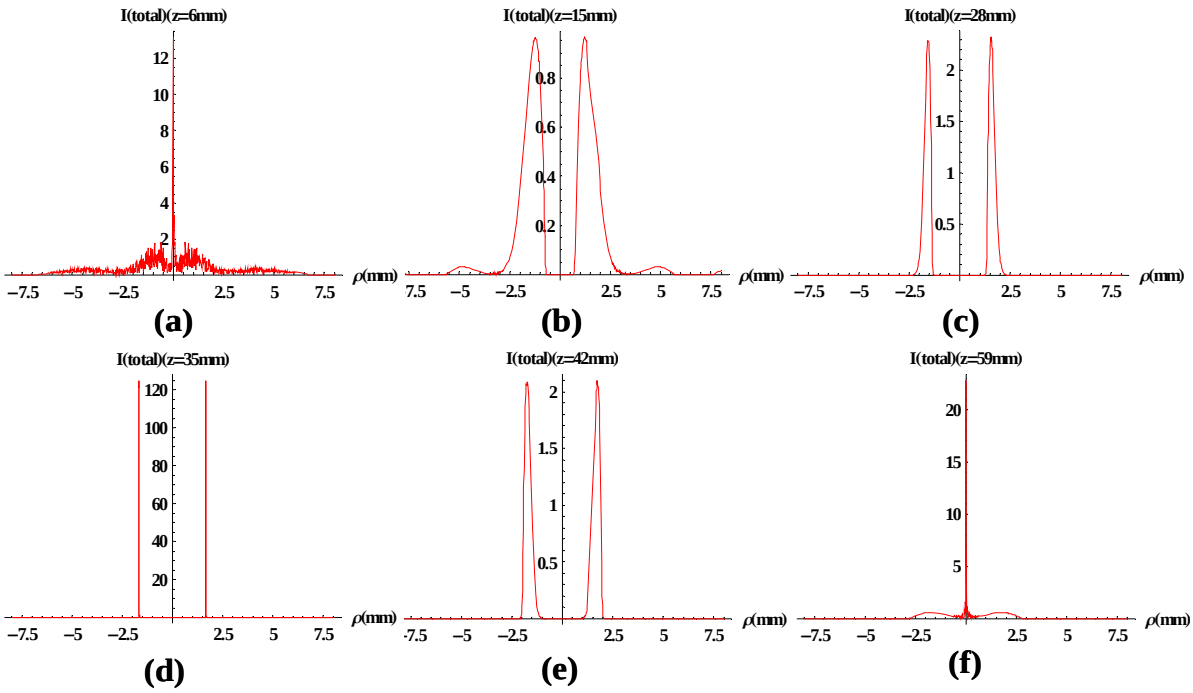

Figure 5.1 Beam profiles of $\gamma = 5^0$ and $f = 35.08$ mm at various propagation distance: (a) z = 6 mm, (b) z = 15 mm, (c) z = 28 mm, (d) z = 35 mm, (e) z = 42 mm, and (f) z = 59 mm.

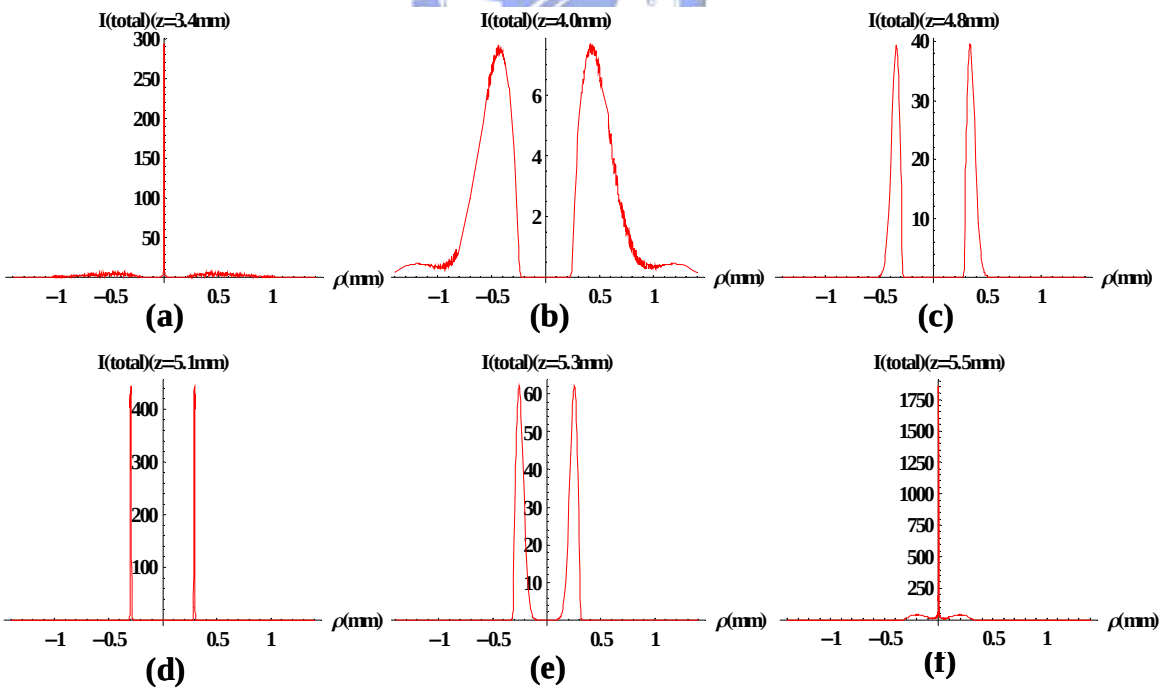

Figure 5.2 Beam profiles of $\gamma = 0.5^0$ and $f = 5.08$ mm at various propagation distance: (a) z = 3.4 mm, (b) z = 4.0 mm, (c) z = 4.8 mm, (d) z = 5.1 mm, (e) z = 5.3 mm, and (f) z = 5.5 mm.

Other than the positions and ranges of bottle beams listed and discussed above, we found the position of the thinnest ring and diameter are at z = 35 mm (Figure 5.1(d)) and 3.34 mm, respectively calculated by using the vectorial diffraction method for condition (1). It is closed to the experimental results that the position at z = 34.12 mm and the diameter is 2.65 mm. Besides, the diameter of the condition (2) is 0.60 mm at z = 5.1 mm as shown in Figure 5.2 (d). From the above discussions, the stimulated results of vectorial diffraction method maybe have some discrepancies of bottle points compared to the scalar diffraction's due to the paraxial approximation. But the key points in use of vectorial diffraction method are the longitudinal field (E_z) considered and comparisons of specific input polarization field. And these detail results would be discussed in the next subsection.

5.2 Comparisons of Specific Input Polarization Field

From the vectorial diffraction integrals of radially and linearly *x*-polarized input fields, the major difference between them is the integral formula that of the *x*-polarized input field depends on the observed angle β. Figure 5.3 and Figure 5.4 show the on-axis intensity versus propagation distance of bottle ranges of radially and linearly x-polarized light for $\gamma = 5^0$ and f = 35.08 mm as well as $\gamma = 0.5^0$ and f = 5.08 mm, respectively. It is understandable that the ranges of bottle beam formed by both radial and linear polarizations are basically the same because of imaging light beam is independent of the direction of polarization. Therefore, we will discuss the transverse and longitudinal field components of two input polarizations in the range of bottle beam in the following.

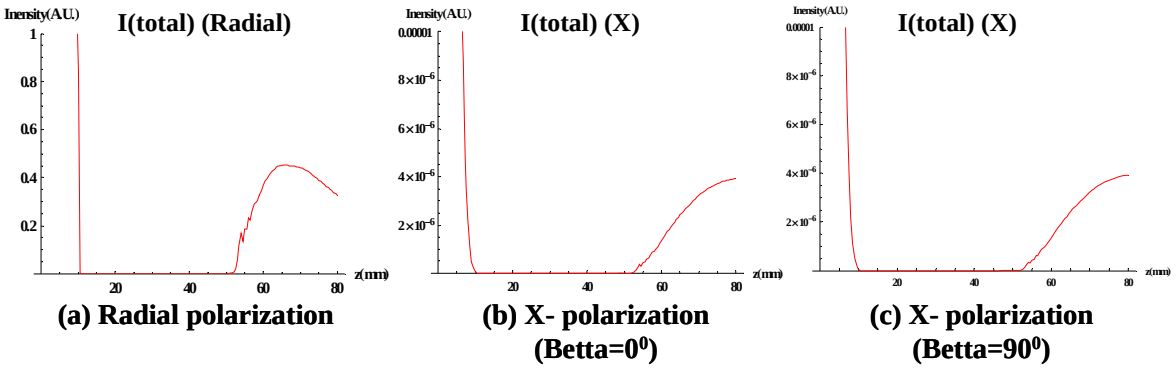

Fig. 5.3 On-axis intensity versus propagation for $\gamma = 5^0$ and $f = 35.08$ mm with radial- and x-polarization at observed angle $\beta = 0^0$, and x-polarization at $\beta = 90^0$.

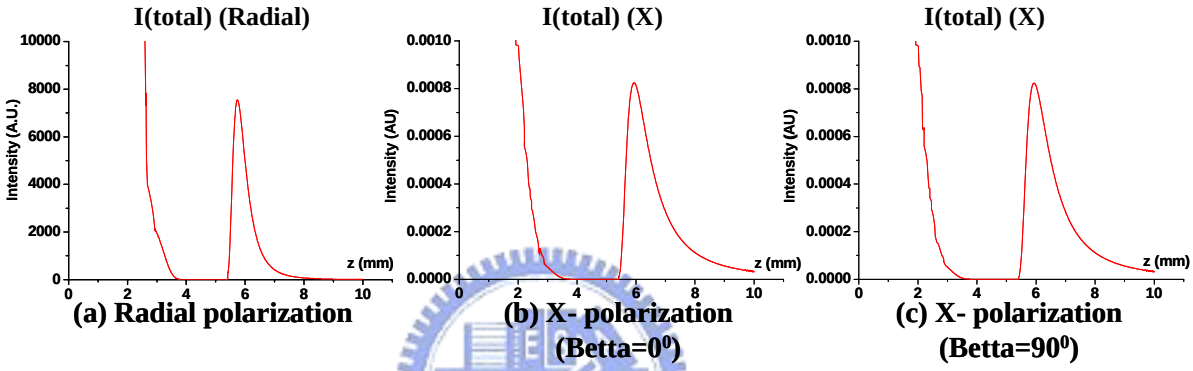

Fig. 5.4 On-axis intensity versus propagation for $\gamma = 0.5^0$ and $f = 5.08$ mm with radial- and x-polarization at observed angle $\beta = 0^0$, and x-polarization at $\beta = 90^0$.

Since an EM wave in the near-field regime is not necessary a transverse wave, we plotted the intensity profiles of transverse and longitudinal fields for the nearby thinnest ring position (Z_b) at z = 37 mm respectively in Figure 5.5 and Figure 5.6 for $\gamma = 5^0$ and $f =$ 35.08 mm. For radial polarized input, we found both cylindrical symmetry for both of the transverse [I_ρ in Figure 5.5(a)] and longitudinal [I_z in Figure 5.5(b)] components; whereas, for the x-polarized input, other than x-polarization is still cylindrical symmetry (Figure 5.6(a)), the angle distribution of y- (Figure 5.6(b)) and z-components (Figure 5.6(c)) follow $\sin^2 2\beta$ and $\cos^2\beta$, respectively.

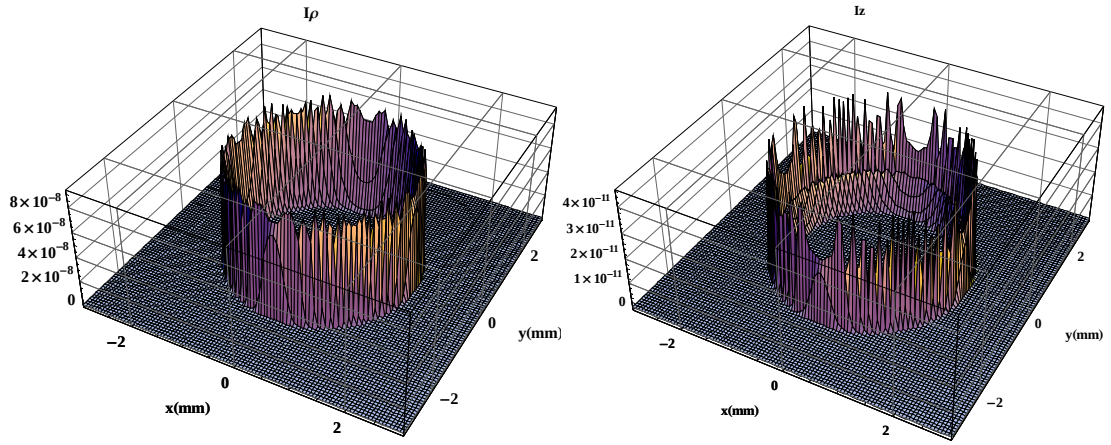

(a) Radial polarization (I ρ =Ix+Iy)

(b) Radial polarization (Iz)

Fig. 5.5 Cross sectional 3D beam profiles of radial polarization at z = 37 mm for $\gamma = 5^0$ and f = 35.08 mm: (a) I_ρ and (b) I_z.

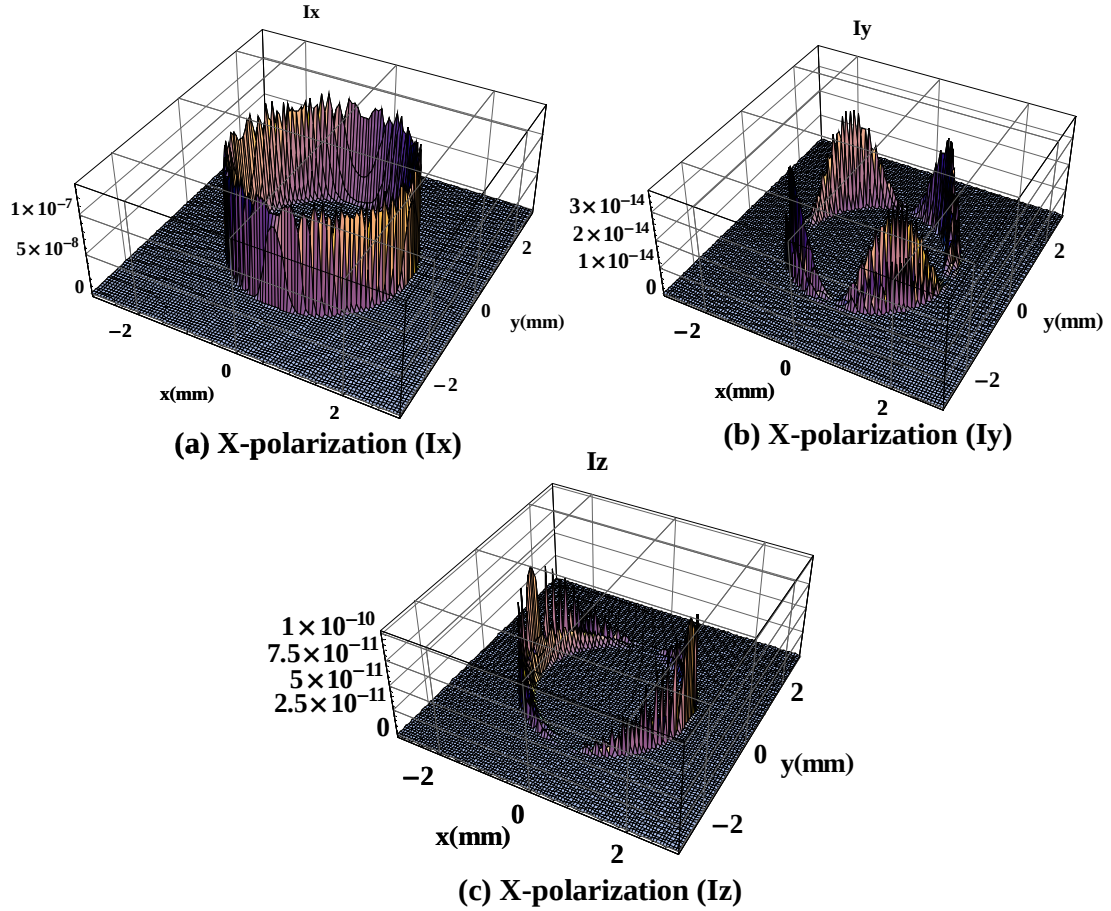

(a) X-polarization (Ix)

(b) X-polarization (Iy)

(c) X-polarization (Iz)

Fig. 5.6 Cross sectional 3D beam profiles of x-polarization at z = 37 mm for $\gamma = 5^0$ and f = 35.08 mm: (a) I_x , (b) I_y , and (c) I_z.